PAPER
Ravi Kumar Pujala *et al.*
Physically crosslinked poly(methacrylic acid-*co*-acrylamide)/
gelatin–chitosan (poly-MAGC) interpenetrating polymer
network hydrogels for drug delivery and antibacterial activity

ROYAL SOCIETY
OF CHEMISTRY

PAPER

Check for updates

Physically crosslinked poly(methacrylic acid-*co*-acrylamide)/gelatin–chitosan (poly-MAGC) interpenetrating polymer network hydrogels for drug delivery and antibacterial activity

Anilkumar Yamala, [ID] [a] Rathangpani Pandit, [b] Ravi Kumar Kanaparthi, [ID] [c] Prasanna Katti, [ID] [b] Sivakumar Vallabhapurapu [ID] *[b] and Ravi Kumar Pujala [ID] *[a]

The pursuit of effective wound healing strategies has driven the development of advanced drug delivery systems that utilize biomaterials to enhance tissue regeneration and control infections. Here we present the synthesis and characterization of a novel interpenetrating polymer network (IPN) hydrogel, comprising poly(methacrylic acid-*co*-acrylamide)/gelatin–chitosan (poly-MAGC). This hydrogel is designed to be biocompatible, biodegradable, and mechanically robust. Its synthesis was achieved *via* physically crosslinked thermally induced free radical polymerization using methacrylic acid (MAA) and acrylamide (AAm) as monomers, in combination with gelatin and chitosan, with potassium persulfate (KPS) as the initiator. A thorough characterization was conducted using field emission scanning electron microscopy (FESEM) to analyze morphology and Fourier-transform infrared (FTIR) spectroscopy to confirm the structural composition and chemical identity of functional groups. Drug release experiments were performed with carbenicillin, a hydrophilic antibiotic, as a model therapeutic agent. The poly-MAGC hydrogel exhibited controlled and pH-responsive drug release, whereas the unloaded hydrogel showed no inherent bactericidal activity against *E. coli* DH5α and *E. faecalis*. Conversely, carbenicillin-loaded hydrogels revealed significant antibacterial properties against *E. coli* DH5α. Notably, unlike previously documented acrylic- or chitosan-based hydrogels, poly-MAGC uniquely combines both synthetic (MAA, AAm) and natural (gelatin, chitosan) polymers through physical crosslinking, avoiding toxic chemical crosslinkers, and achieving a high drug loading efficiency of 89%, enhanced pH-responsive swelling, and remarkable mechanical stability. This synergistic design presents clear advantages over traditional PAA/PMAA or gelatin-only systems, which frequently experience issues with stability or uncontrolled release. Overall, these results position poly-MAGC as a promising multi-functional material for wound dressing, facilitating controlled drug delivery and effective healing.

Introduction

The increasing demand for advanced drug delivery and wound management systems has catalyzed significant research into the development of innovative biomaterials. Traditional methods of drug administration often fall short in achieving localized, sustained, and controlled delivery of therapeutic agents.[1] Advanced biomaterials, such as hydrogels, have emerged as

promising candidates for drug delivery applications due to their ability to retain large volumes of water, mimic the extracellular matrix, and facilitate the controlled release of bioactive molecules. Hydrogels are three-dimensional, cross-linked polymeric networks capable of absorbing substantial quantities of water without dissolving.[2] These materials are synthesized from monomers and polymers containing functional groups such as –NH$_2$, –COOH, –OH, and –SH, which enable hydrogen bonding and electrostatic interactions.[3] Among these, polymers such as polyacrylic acid and poly-methacrylic acid are particularly appealing due to their unique physicochemical properties, including excellent hydrophilicity, pH responsiveness, and biocompatibility. The inclusion of carboxylic acid groups in their structure allows for ionization-dependent behavior, enhancing their versatility in biomedical applications.[4–7] Acrylamide is another widely used monomer in

[a] *Soft and Active Matter Group, Department of Physics, Indian Institute of Science Education and Research (IISER) Tirupati, Yerpedu Mandal, Tirupati, Andhra Pradesh, 517619, India. E-mail: pujalaravikumar@iisertirupati.ac.in*

[b] *Department of Biology, Indian Institute of Science Education and Research (IISER) Tirupati, Yerpedu Mandal, Tirupati, Andhra Pradesh, 517619, India. E-mail: vallabsr@labs.iisertirupati.ac.in*

[c] *Department of Chemistry, Central University of Kerala, Tejaswini Hills, Periye PO, Kasaragod – 671 320, Kerala, India*

hydrogel synthesis, offering amide functional groups that promote robust interactions within the polymer matrix. Hydrogels derived from acrylamide exhibit remarkable properties such as non-toxicity, biocompatibility, and long-term stability *in vivo*, making them ideal candidates for tissue engineering and wound care.[8,9] Combining acrylamide and acrylic acid provides the added advantage of creating interpenetrating network hydrogels with enhanced mechanical strength and tunable drug release profiles.[10,11] Incorporating natural polymers such as gelatin and chitosan into hydrogel systems further augments their biocompatibility and functional properties. Gelatin, derived from collagen, supports cellular adhesion, proliferation, and differentiation, making it a valuable component in biomedical applications. However, gelatin-based hydrogels are prone to dissolution under physiological conditions, necessitating structural reinforcement.[8,12–14] Chitosan, a naturally occurring cationic polysaccharide, complements gelatin by providing antimicrobial activity, adhesive properties, and biodegradability. Modifications to chitosan, such as the introduction of carboxymethyl groups, enhance its solubility and crosslinking potential, enabling the formation of hydrogels with improved network structure, and mechanical and biological properties.[15–20] Recent research has underscored the promise of peptide-based hydrogels and multicomponent hybrid systems in the realm of biomedical applications.[21] For example, supramolecular peptide hydrogels demonstrate remarkable biocompatibility and adjustable biofunctionality, rendering them appealing scaffolds for tissue regeneration and drug delivery. In a similar vein, multicomponent hydrogel systems that combine synthetic and natural polymers offer improved mechanical strength, bioactivity, and responsiveness to stimuli.[22,23] These developments highlight the necessity of creating multifunctional, reproducible hydrogel matrices. Nevertheless, numerous challenges persist regarding structural stability, reproducibility, and the sustained delivery of therapeutics.

Building upon these insights, this study introduces a novel composite hydrogel, poly-MAGC, which integrates the advantages of synthetic polymers (MAA and acrylamide) with natural biopolymers (gelatin and chitosan). This unique combination seeks to address the limitations of existing hydrogel systems by providing a matrix with superior mechanical stability, biocompatibility, and antimicrobial efficacy. "Unlike previously reported acrylic or chitosan-based hydrogels, poly-MAGC integrates both synthetic (MAA, AAm) and natural polymers (gelatin, chitosan) through physical crosslinking without toxic crosslinkers, achieving high drug loading efficiency (89%), superior pH-responsive swelling, and mechanical stability. This synergy makes it more advantageous than conventional PAA/PMAA or gelatin-only systems, which often suffer from poor stability or uncontrolled release". The hydrogel's potential for controlled drug release and its antibacterial activity were investigated using *E. coli* DH5α and *E. faecalis* as a model pathogens, with carbenicellin (CB) serving as the therapeutic agent. The comprehensive characterization and *in vitro* evaluation of this hydrogel establish its promise as a next-generation wound dressing material.

Results and discussions

Synthesis of poly-MAGC hydrogel

The hydrogel was prepared through a free radical polymerization process involving monomers methacrylic acid (MAA) and acrylamide (AAm), in the presence of the radical initiator potassium persulfate (KPS). The polymerization process begins when the unpaired electron generated by KPS is transferred to the monomer units, activating them and initiating the chain reaction for polymerization.[24] During the reaction, crosslinking occurs alongside polymerization to form a three-dimensional network. The process was carried out for an hour under controlled conditions to ensure complete polymerization and crosslinking. The inclusion of gelatin in the formulation contributed to the development of hydrophobic domains within the hydrogel matrix. These domains act as durable crosslinking sites, enhancing the structural stability of the hydrogel.[15,25] Chitosan, with its intrinsic cationic properties, interacted with the anionic functional groups of MAA and AAm, forming polyelectrolyte complexes. This interaction not only improved the mechanical integrity of the hydrogel but also imparted tunable properties such as enhanced swelling behavior, pH responsiveness, and biocompatibility. These characteristics make the hydrogel suitable for various biomedical applications.[26,27]

The hydrogel was synthesized *via* free radical polymerization using methacrylic acid (MAA) and acrylamide (AAm) as monomers, with potassium persulfate (KPS) as the radical initiator. Polymerization was initiated when KPS generated free radicals, activating monomer units and triggering a chain reaction. Simultaneously, network formation occurred through a combination of physical crosslinking mechanisms, ensuring a stable hydrogel structure without the need for di-functional chemical crosslinkers like MBA. The three-dimensional network formation in our system is primarily driven by hydrogen bonding and electrostatic interactions, thermal gelation of gelatin, thermal polymerization of MAA and AAm, and chitosan's role in enhancing crosslinking. Chitosan ($-NH_2$), gelatin ($-COOH$, $-NH_2$), methacrylic acid ($-COOH$), and acrylamide ($-CONH_2$) interact through hydrogen bonding and electrostatic forces, forming a physically crosslinked network. Additionally, gelatin undergoes a sol–gel transition upon heating and cooling, contributing to the network's stability. At 70 °C, methacrylic acid and acrylamide undergo thermal polymerization, forming entangled polymer chains with chitosan and gelatin, further strengthening the matrix. Chitosan enhances the network through hydrogen bonding and electrostatic interactions with gelatin and synthetic polymer chains, creating a stable structure without the need for toxic chemical crosslinkers.[28–30]

Chitosan is typically insoluble in pure water and at basic pH due to the deprotonation of its amino groups. To ensure proper solubilization, chitosan was initially dissolved in a 2% (v/v) acetic acid solution, allowing complete protonation. The addition of NaOH was carefully controlled to neutralize MAA and adjust the pH of the final hydrogel mixture while ensuring that chitosan remained in a soluble or gel-like state. The final pH

range was optimized to allow chitosan to participate in electrostatic interactions with the anionic groups of MAA, even in a partially protonated state. The formation of polyelectrolyte complexes and the stable hydrogel network was confirmed *via* FTIR analysis, which demonstrated a broad peak in the O–H stretching region, distinguishing the final hydrogel from its monomeric precursors. These findings validate the successful integration of chitosan and gelatin into the hydrogel matrix, contributing to its enhanced mechanical integrity and tunable properties such as swelling behavior, pH responsiveness, and biocompatibility.[16–18,31]

FTIR and FESEM analysis

The FT-IR spectra provide critical insights into the structural composition and chemical interactions within the poly-MAGC hydrogel (Fig. 2A). The spectrum displays a broad absorption band at 3437 cm^{-1} and 3228 cm^{-1}, attributed to O–H and N–H stretching vibrations. These signals also indicate intermolecular hydrogen bonding between protein and polysaccharide components, highlighting the hydrogel's composite nature. Such bonding plays a crucial role in stabilizing the network and influencing its swelling and mechanical properties. Additionally, the spectrum features a band at 1050 cm^{-1}, corresponding to C–OH stretching in the glucopyranose ring, a key structural component of polysaccharides. This suggests the presence of carbohydrate-based polymers, such as chitosan, which contribute to the hydrogel's biocompatibility and antimicrobial properties. For the pure PMAA hydrogel, a broad peak spanning 3660–3000 cm^{-1} reflects O–H and N–H stretching vibrations, reinforcing the role of hydroxyl and amine groups in maintaining hydrophilicity and intermolecular interactions. The peak at 2940 cm^{-1} is ascribed to C–H stretching in the –CH$_2$ group, signifying the hydrocarbon framework of the polymer matrix. Moreover, two prominent FTIR absorption bands observed at 1692 cm^{-1} and 1258 cm^{-1} correspond to the stretching vibrations of the C=O (carbonyl) and C–O (carboxylate) functional groups, respectively. These functional moieties, in conjunction with –NH$_2$ groups present in the hydrogel matrix, are instrumental in imparting pH-responsive behavior. Their protonation and deprotonation under varying pH conditions modulate hydrogel swelling, drug-polymer interactions, and ultimately control drug release dynamics in the physiological and tumor microenvironments. Further analysis reveals peaks at 1489 cm^{-1} and 1368 cm^{-1}, attributed to CH$_2$ and CH$_3$ deformations, respectively, which emphasize the structural complexity of the hydrogel. Lastly, a band around 1166 cm^{-1}, assigned to C–N stretching, confirms the presence of amide bonds, indicative of gelatin incorporation into the hydrogel.

These spectral features collectively demonstrate the successful integration of synthetic and natural polymers within the hydrogel, establishing its multifunctional properties. The detailed identification of functional groups explains the hydrogel's biocompatibility, swelling behavior, and controlled drug delivery capability, aligning with its intended biomedical applications. This comprehensive characterization also provides a

foundation for optimizing the hydrogel for specific therapeutic and regenerative uses.

The surface morphology of the poly-MAGC hydrogels was examined using field emission scanning electron microscopy (FESEM) to assess the structural characteristics and their potential influence on hydrogel properties. The FESEM images (Fig. 1E) revealed a non-uniform, corrugated surface structure for the hydrogel sample. This surface topology is crucial as it can influence the hydrogel's performance in various biomedical applications, such as drug delivery and tissue engineering.[32] In Fig. 1(E), the copolymer hydrogel exhibited a mesoporous structure. This smoothness is indicative of the base hydrogel formulation, which maintains a stable and uniform structure.

^{1}H NMR analysis

The successful polymerization of methacrylic acid and acrylamide in the poly-MAGC hydrogel was confirmed by ^{1}H NMR spectroscopy using methanol-d_4 as the solvent. This technique enables the identification of characteristic chemical shifts associated with the monomers and their disappearance upon polymerization. In the spectra, the absence of vinyl proton signals typically found between 5.5–6.5 ppm, corresponding to the –C=CH$_2$ groups of the monomers, indicates the consumption of double bonds during free-radical polymerization. In contrast, the poly-MAGC hydrogel exhibited broad peaks in the range of 1.15–2.7 ppm, specifically at 1.18 ppm (–CH$_3$), 2.25 ppm (–CH), and 2.7 ppm (–CH$_2$), which are characteristic of the saturated aliphatic protons in the polymer backbone (Fig. 2B). These spectral features confirm the successful conversion of monomeric double bonds into single bonds, validating the formation of the intended polymer network.

BET analysis

The porous architecture of the freeze-dried poly-MAGC hydrogel was thoroughly characterized using nitrogen adsorption–desorption isotherms at 77 K. The BET analysis revealed a high specific surface area of 394.67 m^2 g^{-1}, suggesting the formation of a highly porous structure (Fig. 2E). This significant surface area is attributed to the synergistic combination of natural polymers (gelatin and chitosan) with synthetic monomers (methacrylic acid and acrylamide), which together form an interconnected polymeric network during polymerization and freeze-drying. Complementary BJH analysis (Fig. 2D) further confirmed a total pore volume of 2.26 cm^3 g^{-1} and a pore radius distribution ranging from ~1.5 nm to over 20 nm, indicating a predominantly mesoporous structure with contributions from macropores.[33,34]

The nitrogen adsorption isotherm (Fig. 2C) exhibited a typical type IV pattern with a hysteresis loop, characteristic of mesoporous materials, supporting the presence of capillary condensation within the pores.[35] These morphological features enhance the hydrogel's ability to interact with and retain small molecules, making it especially suitable for controlled drug delivery, cellular infiltration, and pollutant adsorption. The combination of high surface area, well-distributed pore size, and strong BET correlation ($r = 0.9956$) confirms the structural
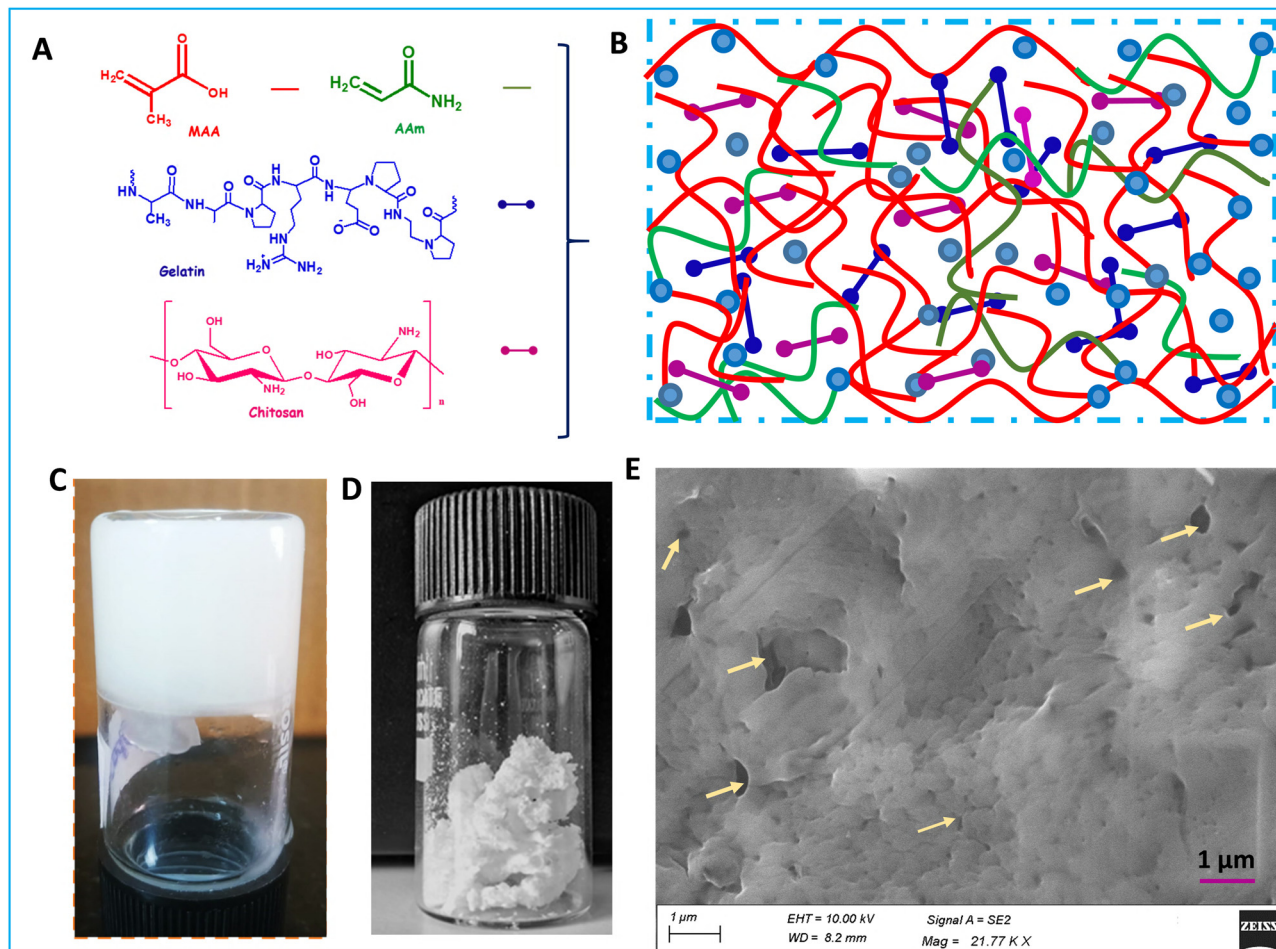
Fig. 1 Synthesis, structure, and morphological characterization of poly-MAGC hydrogel. (A) Chemicals used as precursors for the hydrogel synthesis. (B) Illustration of hydrogel formation through crosslinking and intramolecular attractions, demonstrating the structural network of the hydrogel (The red and green curves represent the polymers of methacrylic acid (MAA) and acrylamide (AAm), while the blue and pink symbols denote gelatin and chitosan, respectively. Additionally, the blue circles indicate the presence of water). (C) Camera image of the prepared poly-MAGC hydrogel, showcasing its physical appearance. (D) Image of the freeze-dried hydrogel. (E) Field Emission scanning electron microscopy (FESEM) image of the poly-MAGC hydrogel, revealing its microstructure and porous network.

integrity and functional versatility of the poly-MAGC hydrogel, positioning it as a promising candidate for biomedical applications such as tissue engineering and drug release systems, as well as for environmental remediation.[36]

Swelling nature

The swelling experiments were conducted at rest without stirring to mimic real-world conditions where the hydrogel would be used in a static environment. The hydrogel's water absorption is primarily influenced by the presence of hydrophilic functional groups such as –COOH, –NH$_2$, and –C=O within its polymer structure (Fig. 3A). These groups actively interact with water molecules, enabling the material to exhibit significant swelling behavior.[37,38] The swelling ratio demonstrates a strong dependency on the surrounding pH, with the highest swelling observed at pH 8.4. This pH-responsive behavior is directly related to the ionization states of the functional groups in the polymer network.[39] At alkaline pH levels, the –COOH groups undergo deprotonation, increasing the negative

charge density within the hydrogel. This results in enhanced electrostatic repulsion between polymer chains and greater water influx into the network.[40] Conversely, at acidic pH levels, the protonation of amino groups (–NH$_3^+$) increases their hydrophilicity, while the protonation of carboxyl groups (–COOH) reduces their hydrophilicity and creating a more compact hydrogel structure. The protonated groups generate stronger hydrogen bonding and hydrophobic interactions, which limit water absorption and reduce the swelling ratio.[10] The hydrogel's swelling behavior is influenced not only by pH but also by external environmental factors such as temperature, ionic strength, and the presence of electrolytes.[41] For instance, in deionized water, the absence of counter ions allows the hydrogel to swell freely as there is minimal interference with the electrostatic forces between the charged polymer chains. However, in phosphate-buffered saline (PBS) or biological fluids, the abundance of ions influences the hydrogel more swell. The observed swelling ratio across different pH environments follows this trend:
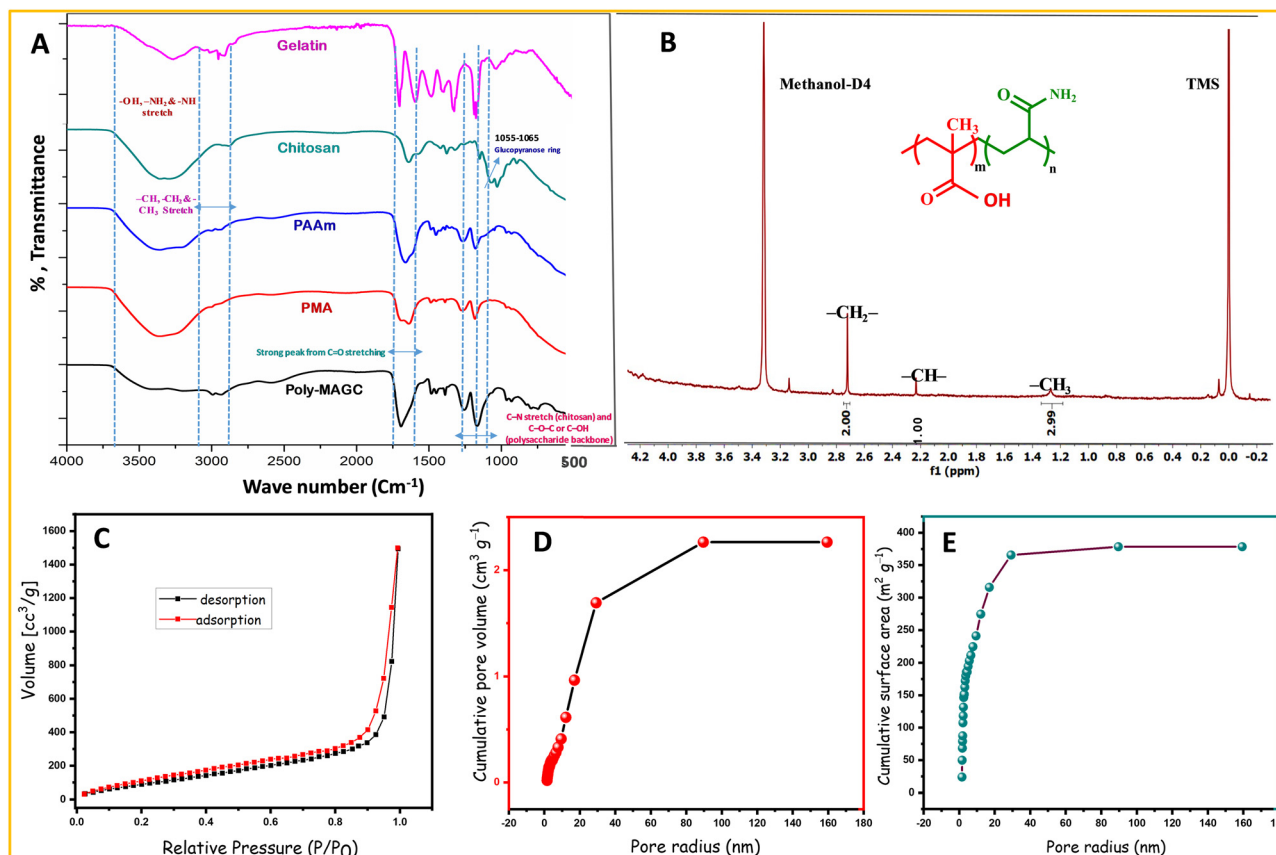
Fig. 2 Characterization of poly-MAGC hydrogel: functional group analysis and structural confirmation. (A) FTIR spectra of gelatin, chitosan, PMAAm, PMAA, and poly-MAGC showing characteristic functional group vibrations and confirmation of successful interpenetrating network formation. (B) ^{1}H NMR spectrum of poly(methacrylic acid-co-acrylamide) recorded in CD$_3$OD, illustrating the disappearance of vinyl proton peaks and the presence of saturated backbone signals, confirming successful polymerization; the polymer structure is shown inset. Characterization of mesoporous material structure: (C) nitrogen adsorption–desorption isotherm at 77 K showing type IV behavior with hysteresis loop, indicative of mesoporosity. (D) Pore size distribution profiles showing cumulative pore volume and surface area (E) as functions of pore radius, with primary peaks in the 2–20 nm range.

pH 4.4 < 5.4 < 7.0 < 8.4 < 7.4 (PBS).

The compact structure and reduced hydrophilicity at low pH levels contribute to the hydrogel's stability under acidic conditions. Meanwhile, the higher swelling ratio at neutral and alkaline pH levels highlights its potential responsiveness in biological environments. The results demonstrate that the hydrogel not only remains structurally stable but also responds dynamically to external pH changes. This tunable swelling behavior is crucial for applications such as drug delivery systems, tissue engineering scaffolds, and wound care materials, where responsiveness to environmental conditions is key to their functional performance.[42] The observed slow mass loss at acidic pH may be attributed to the protonation of carboxylate groups, which reduces electrostatic repulsion, increases the solubility of protonated chitosan (–NH$_3^+$), and disrupts hydrogen bonding within the hydrogel network.

Surface wettability (contact angle analysis)

The analysis of the contact angle (Fig. S1(A–D) and Table S1) demonstrated the highly hydrophilic characteristics of the poly-MAGC hydrogel. At the initial measurement of 6 seconds, the hydrogel displayed a contact angle of approximately 37°,

suggesting a degree of resistance to spreading due to the reorganization of hydrophilic domains. Nevertheless, this angle significantly decreased to around 18° after 120 seconds, indicating rapid water spreading and absorption within the hydrogel matrix. This reduction over time illustrates the hydrogel network's strong affinity for water, which is attributed to the presence of numerous polar functional groups (–COOH, –CONH$_2$, –NH$_2$) from MAA, AAm, gelatin, and chitosan. The remarkable wettability observed underscores the hydrogel's potential for biomedical applications, including wound dressings and drug delivery systems, where effective hydration and contact with tissues are crucial.

Water retention nature

The water retention capability of the hydrogel is closely linked to its swelling behavior and is influenced by environmental pH (Fig. 3B). Water retention reflects the hydrogel's ability to maintain absorbed water under ambient conditions, which is critical for applications in drug delivery and wound healing where sustained hydration is essential. The hydrogel's water retention ratio (WRR) was evaluated across different pH levels,
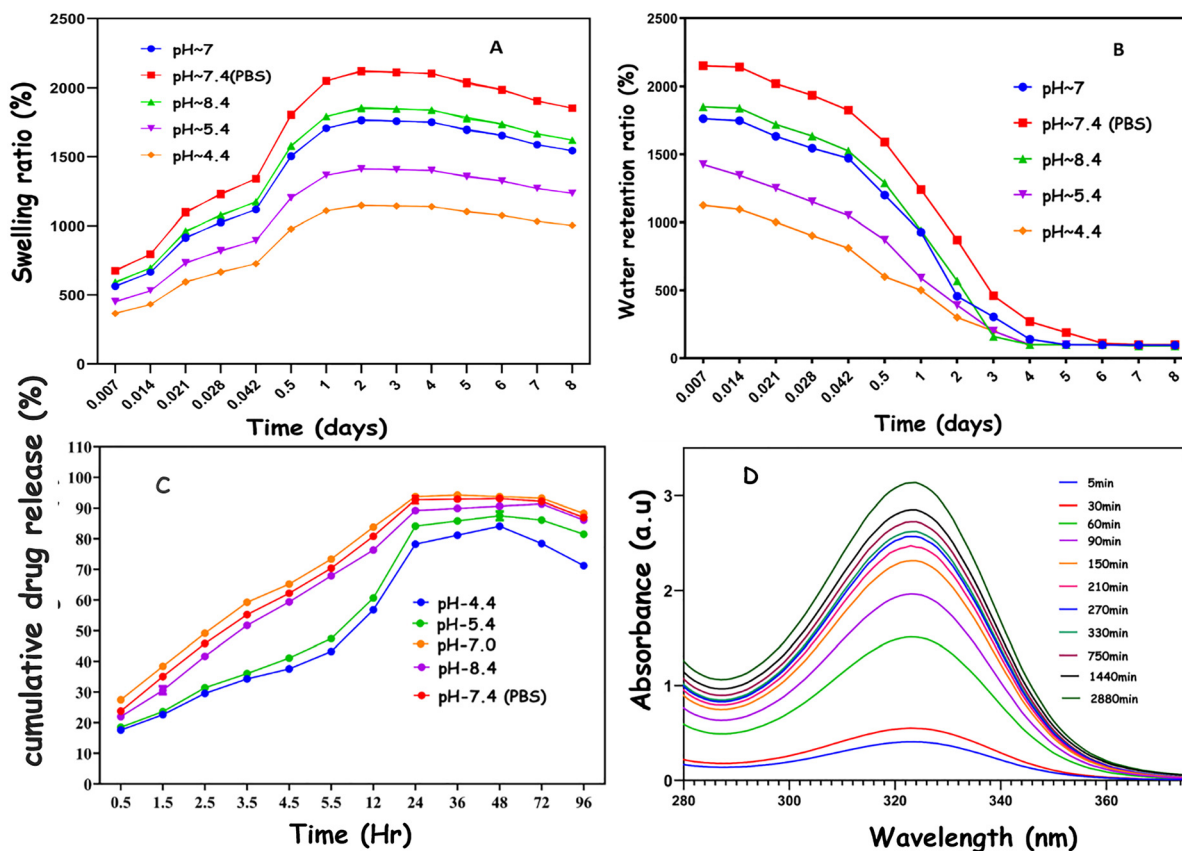
Fig. 3 pH-dependent hydrogel characterization of swelling, water retention and drug release kinetics: (A) Swelling behavior of poly-MAGC hydrogels at different pH levels over time, demonstrating pH-responsive swelling due to ionizable functional groups within the polymer network. (B) Water retention capacity of the hydrogels under ambient conditions, indicating the hydrogel's ability to retain absorbed water over an extended period. (C) Carbenicillin release kinetics from poly-MAGC hydrogels at different pH environments, showing sustained and pH-sensitive release profiles. (D) UV-vis absorption spectra of cumulative drug release at pH-7 and at room temperature (λ = 322 nm).

specifically pH 4.4, 5.4, 7.0, 7.4 (PBS), and 8.4, following swelling experiments. The WRR is significantly impacted by the pH-dependent structure of the hydrogel, which alters the density and stability of the water-binding functional groups such as –COOH and –NH$_2$.[43] At low pH levels (pH 4.4 and 5.4): The hydrogel exhibits compact and hydrophobically dominant structures due to the protonation of the –COOH and –NH$_2$ groups. This tight network restricts water loss, resulting in moderate water retention.[43] However, the reduced hydrophilicity limits the swelling capacity, which inherently constrains the volume of water retained.[38] At neutral pH (pH 7.0 and PBS): The hydrogel demonstrates increased swelling due to partial ionization of the –COOH groups, enhancing electrostatic repulsion and hydration. While water retention improves compared to acidic conditions, the presence of counter ions in PBS leads to charge screening, which slightly reduces the WRR compared to pure neutral pH solutions. At alkaline pH levels (pH 8.4): The deprotonation of –COOH groups results in maximal electrostatic repulsion, creating a highly expanded hydrogel network. This open structure allows for high water absorption during swelling, but it also makes the hydrogel more prone to water loss under ambient conditions, reducing WRR compared to pH 7.4 (PBS). The trend in water retention across different

pH conditions aligns with the swelling behavior, following the order:

$$\text{pH } 4.4 < 5.4 < 7.0 < 8.4 < 7.4 \text{ (PBS)}.$$

This behavior underscores the hydrogel's ability to retain water efficiently under physiological pH (7.4, PBS), making it well-suited for biomedical applications where maintaining hydration is crucial. Furthermore, the ability to modulate water retention by adjusting environmental pH enhances the versatility of the hydrogel for controlled release systems and wound care, ensuring an optimal balance between hydration and structural integrity under various conditions.

Crosslinking density analysis using Flory–Rehner theory

To quantitatively validate the tightly cross-linked nature of the hydrogel as claimed in the enzymatic degradation section, the crosslinking density (ν_e) was calculated using the Flory–Rehner equation. Swelling ratio data obtained at various pH values was used to determine the polymer volume fraction, from which ν_e was derived.[6] The swelling ratios at pH 4.4, 5.4, 7.0, 7.4, and 8.4 were 1000%, 1240%, 1680%, 2200%, and 1720%, respectively. Corresponding crosslinking densities were calculated to be

3.68×10^{-5}, 2.11×10^{-5}, 9.61×10^{-6}, 4.74×10^{-6}, and 9.03×10^{-6} mol cm^{-3}. These results reveal an inverse relationship between pH and crosslinking density, with the lowest density observed at pH 7.4, corresponding to maximum swelling. This suggests that the hydrogel network becomes more expanded under physiological conditions, likely due to deprotonation of functional groups leading to enhanced electrostatic repulsion. The higher crosslinking density at acidic pH (4.4 and 5.4) supports the claim of a more compact and stable network structure in low-pH environments, thereby validating the hydrogel's pH-responsive behavior and structural integrity under enzymatic and acidic conditions. Such pH-tunable network characteristics are essential for applications like controlled drug release and targeted delivery in specific biological environments.

Carbenicillin (CB) loading efficiency in poly-MAGC hydrogel

CB, a widely recognized antibacterial agent, is commonly used for treating various bacterial infections. In this study, CB was selected as a representative compound to evaluate the efficiency of poly-MAGC based hydrogels as drug delivery systems. The incorporation of CB into the hydrogel matrix was achieved through electrostatic interactions between the charged components of the hydrogel and CB molecules. CB, being a water-soluble drug, is encapsulated within the hydrogel matrix through a combination of mechanisms. Firstly, during the swelling process, the hydrogel absorbs water and expands, allowing drug molecules to diffuse into its porous polymeric network where they become physically entrapped; the extent of encapsulation is influenced by factors like porosity, mesh size, and swelling degree. Secondly, electrostatic interactions play a significant role, especially when the hydrogel contains ionizable functional groups such as –COOH, –NH$_2$, which can attract oppositely charged drug molecules—for instance, anionic hydrogels encapsulate cationic drugs *via* electrostatic attraction. Lastly, hydrogen bonding and hydrophilic interactions contribute to stabilization, as functional groups like –OH, –COOH, and –NH$_2$ form hydrogen bonds with the drug, enhancing retention and reducing premature diffusion from the hydrogel. These combined interactions enhance drug loading efficiency and help modulate its controlled release. The hydrogels demonstrated a drug-loading capacity of 0.0393 M, highlighting their ability to encapsulate the antimicrobial agent effectively. Using calculations based on eqn (3), it was determined that the CB loading efficiency of the hydrogel reached an impressive 89%. The swelling characteristics of poly-MAGC were observed to be significantly influenced by pH levels, which in turn affected both the drug loading and release profiles. Under acidic pH conditions, the carboxyl groups present in methacrylic acid remain protonated, which minimizes electrostatic repulsion and limits the expansion of the network. This contracted state leads to a decrease in water absorption, thereby restricting the diffusion and adsorption of hydrophilic drugs. Conversely, at physiological pH (7.0–7.4, PBS), the partial ionization of the –COOH groups generates considerable electrostatic repulsion, resulting in maximum swelling. This

expanded network allows for increased drug loading and a prolonged release profile. In alkaline pH conditions, despite complete ionization, the system undergoes ionic charge screening and partial contraction, which again diminishes swelling and drug release. Supporting this observation, poly-MAGC demonstrated the highest loading efficiency at pH 7.4, achieving a drug loading capacity (LC) of 89% for carbenicillin. This finding confirms that the hydrogel is ideally suited for drug delivery in physiological environments.

Release kinetics in PBS and different pH conditions

The drug release kinetics of CB-loaded poly-MAGC hydrogel were studied using UV-vis spectroscopy at 324 nm to evaluate its encapsulation efficiency and release behavior under various conditions. Release studies conducted in PBS (pH 7.4) showed that approximately 83% of the encapsulated AMP was released within 12 hours at pH ~ 7, with a similar release of $\sim 80\%$ observed at pH ~ 7.4. Sustained release continued up to 72 hours, after which it plateaued due to equilibrium or potential photochemical degradation. The release profile was influenced by pH, with faster release at higher pH levels (7.4–8.4) due to increased hydrogel swelling and functional group deprotonation, while lower pH levels (4.4–5.4) reduced swelling and slowed CB diffusion. The optimal release rate at pH ~ 7.4 aligns with physiological conditions, suggesting suitability for biomedical applications. However, CB stability was found to decrease at low pH and temperatures above 27 °C, with degradation observed in the culture medium within 2–3 days, underscoring the need for controlled environmental conditions. These findings highlight the hydrogel's efficient drug encapsulation and its potential for pH-responsive, controlled drug delivery systems. The drug release profile (0–96 hours) exhibited a classic diffusion-controlled pattern, with an initial rapid release phase (0–2000 min) followed by sustained release and eventual plateau (~ 6000 min). The Higuchi model provided the most accurate fit ($R^2 = 0.98$, $Q_t = 0.11\sqrt{t}$), confirming that the release mechanism is governed by Fickian diffusion through a porous matrix structure, typical of non-swelling, monolithic systems like hydrophobic tablets or inert gels. The Korsmeyer–Peppas exponent ($n = 0.25$, $n < 0.45$) further validated this diffusion dominance, suggesting minimal polymer relaxation or erosion.

Enzymatic degradation

We used collagenase as a primary examination to evaluate the biodegradability of poly-MAGC hydrogel due to the presence of gelatin, a denatured form of collagen rich in peptide and amide bonds that are known targets for collagenase. This enzymatic degradation simulates extracellular matrix (ECM) remodelling, which is crucial in biomedical contexts such as tissue regeneration, drug release, and wound healing. More compact and crosslinked network, impeding enzymatic access and slowing degradation.[19] These findings underscore the tunability of poly-MAGC degradation rates by adjusting hydrogel concentration (Fig. 4). This adaptability is advantageous in designing scaffolds for tissue engineering, where prolonged support is
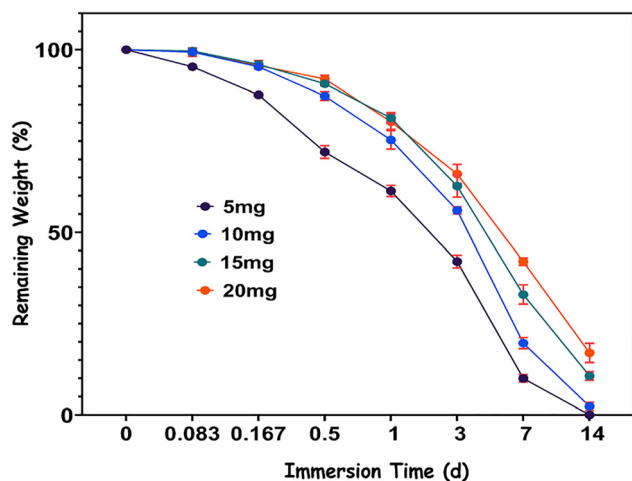
Fig. 4 Collagenase-mediated enzymatic degradation profile of poly-MAGC hydrogel over time. The hydrogel exhibited gradual mass loss upon exposure to collagenase, indicating its biodegradability and enzymatic sensitivity. The degradation behavior underscores the hydrogel's potential in bioresponsive applications, especially in tissue engineering and controlled drug delivery systems. The data presented reflects the mean ± SEM from three independent experiments.

essential, or in drug delivery systems requiring sustained release. While synthetic polymers like PMAA and PAAm are not inherently biodegradable, enzymatic cleavage of the gelatin backbone disrupts the overall network, facilitating partial breakdown and potential elimination of synthetic fragments.[44] Chitosan plays a pivotal role in the biodegradability of hydrogels due to its natural origin, enzymatic sensitivity, and favorable chemical structure. As a polysaccharide derived from chitin, chitosan contains β-(1 → 4)-linked D-glucosamine units, which are readily cleaved by lysozyme, an enzyme abundantly present in human tissues and bodily fluids. This enzymatic degradation pathway is particularly significant in biomedical environments, where chitosan-based materials gradually break down into non-toxic, bioresorbable fragments. Furthermore, the biodegradability of chitosan is influenced by its degree of deacetylation and molecular weight, which modulate its solubility and susceptibility to hydrolysis. In hydrogel formulations, chitosan contributes to matrix erosion through both enzymatic cleavage and pH-responsive behavior; under acidic conditions, the protonated amine groups ($-NH_3^+$) increase solubility, accelerating degradation.[18] Importantly, when chitosan is integrated with other natural polymers such as gelatin or synthetic monomers like methacrylic acid and acrylamide, its degradation facilitates the destabilization of the overall network, enabling controlled breakdown and clearance of the hydrogel system.[20] Thus, the hydrogel demonstrates promising bio-responsiveness and controlled degradability for safe biomedical applications. In this study, poly-MAGC hydrogels of varying concentrations (5, 10, 15, and 20 mg) were incubated in collagenase-containing solutions over periods ranging from 2 hours to 14 days. The degradation rate was inversely proportional to hydrogel concentration. The 5 mg formulation degraded completely within 7 days, while the 10,

15, and 20 mg formulations showed residual weights of 2.3%, 10%, and 17%, respectively, after 14 days. This trend indicates that higher concentrations yield a the poly-MAGC hydrogel network undergoes controlled degradation through the enzymatic breakdown of its natural components (gelatin and chitosan), which destabilizes the crosslinked structure and releases the non-biodegradable synthetic polymers, PMAA and PAAm. Although these synthetic chains resist enzymatic degradation, their fragmentation into low-molecular-weight or water-soluble forms upon network disruption allows for systemic clearance *via* renal filtration or hepatic pathways, depending on their size and solubility. This indirect elimination mechanism—enabled by the degradation of natural polymers—ensures that both the hydrogel's natural and synthetic components are safely removed from the body over time, making the system suitable for biomedical applications such as tissue engineering and drug delivery, where long-term biocompatibility is essential.

Rheology

The rheological analysis of the hydrogel revealed several key findings relevant to its potential in biological applications. In the amplitude sweep test (Fig. 5A), the hydrogel demonstrated a well-defined linear viscoelastic (LVE) region, with the storage modulus (G') remaining stable up to approximately 1% strain. Beyond this point, G' and the loss modulus (G'') began to decline, indicating structural degradation. The ratio of G'/G'' was consistently greater than 1, confirming the dominance of elastic properties and its behavior as a viscoelastic solid. Frequency sweep tests showed that G' exceeded G'' across the tested range (0.01–1000 rad s^{-1}), with a plateau in G' at low frequencies, highlighting the hydrogel's strong elastic nature and structural stability (Fig. 5B).[45] Temperature ramp tests (Fig. 5C) from 25 °C to 60 °C revealed a reduction in G', attributed to increased thermal vibrations and volume expansion, though the hydrogel maintained gel stability under these conditions[46] (Fig. S1A). The primary focus of this study was to evaluate the material's behavior within the biologically relevant temperature range (37 °C to 45 °C), as this is critical for its intended bio applications. The observed rheological properties within this range, including the transition above 50 °C, provide sufficient evidence to support the material's functionality under physiological conditions. At low shear rates, the viscosity stays constant (Newtonian plateau). As shear rate increases, the viscosity drops sharply (shear-thinning region), following a power-law pattern. At very high shear rates, the viscosity levels off again. This behavior is typical of many polymers, gels, and complex fluids, showing how their structure breaks down under flow but can recover when the force is removed. The sharp transition points between these regions reveal important information about the material's internal structure and stability (Fig. S1B). Additionally, the hydrogel exhibited pseudoplastic behavior, transitioning from Newtonian flow at low shear rates to shear-thinning at higher rates, consistent with the entanglement model of semi-flexible hydrogels.[47] The time sweep test results (Fig. 3D) demonstrate the viscoelastic properties of the hydrogel, with the storage modulus (G') consistently
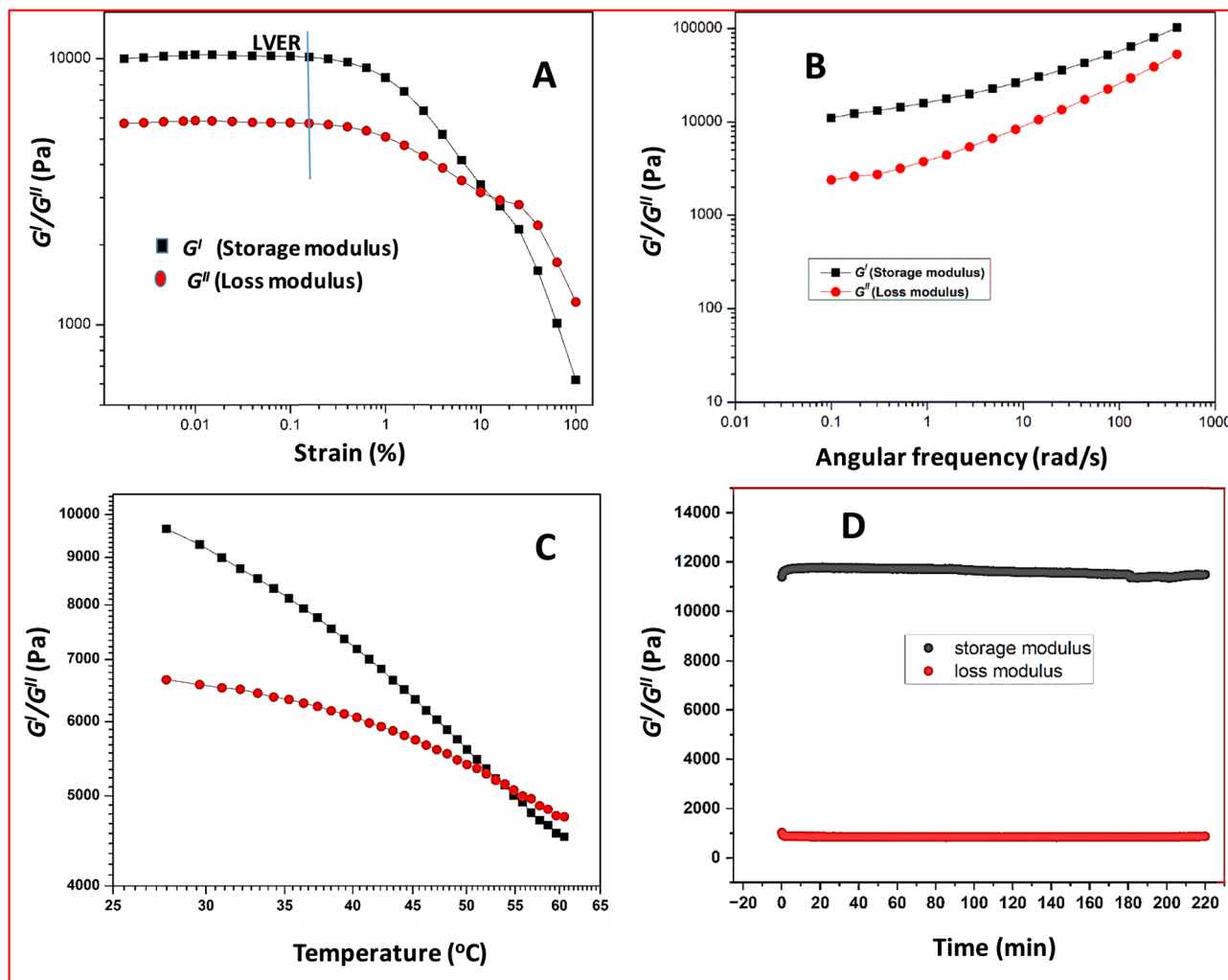
Fig. 5 Rheological characterization of poly-MAGC hydrogel: mechanical stability. (A) Strain sweep analysis of poly-MAGC hydrogel showing the variation of storage modulus (G') and loss modulus (G'') with increasing strain, identifying the linear viscoelastic region (LVER). (B) Frequency sweep analysis illustrating the dependence of storage and loss moduli on angular frequency, demonstrating the hydrogel's solid-like behaviour. (C) Temperature sweep study illustrating the decrease in storage and loss moduli with increasing temperature, suggesting thermal softening of the hydrogel network. (D) Time sweep experiment demonstrating the stability of the hydrogel's mechanical properties under constant strain and temperature over time.

higher than the loss modulus (G'') throughout the 220-unit test period, indicating dominant elastic behavior characteristic of a stable gel network. During the initial phase (0–100 min), both moduli remain nearly constant, reflecting structural integrity and equilibrium, which is crucial for applications requiring short-term mechanical stability, such as drug delivery carriers or tissue scaffolds. Beyond 100 min, the gradual decline in G' suggests progressive network softening, potentially due to hydrolytic or enzymatic degradation, a desirable feature for controlled-release systems but potentially limiting for longterm structural applications. The persistent gap between G' and G'' confirms the material retains its gel state despite softening, highlighting its resilience. These rheological properties align with biomedical uses where balanced stability and degradability are needed, though formulation tweaks (*e.g.*, enhanced crosslinking) could extend functional duration if required. The absence of abrupt modulus drops indicates homogeneous

degradation, favorable for predictable performance in physiological environments. The tunable mechanical properties, with an elastic modulus ranging from approximately 200 Pa to 8000 Pa, make the hydrogel suitable for diverse biomedical uses, from supporting neurite outgrowth on softer matrices to promoting bone marrow stromal cell differentiation on stiffer substrates. Its ability to maintain elasticity and structural integrity under varying environmental conditions reinforces its potential for bone, muscle, and soft tissue engineering, establishing it as a promising candidate for advanced biological research and regenerative medicine.

Metabolic activity through MTT assay

To evaluate the potential biomedical applications of the synthesized poly-MAGC hydrogel, including drug delivery, antibacterial studies, tissue engineering, and wound dressing, cytotoxicity tests were conducted using three distinct cell lines. The

hydrogel was tested on HEK 293T and MCF-7 cell lines to assess its influence on cell viability, a critical parameter for determining the biocompatibility of materials intended for medical applications (Fig. 6).
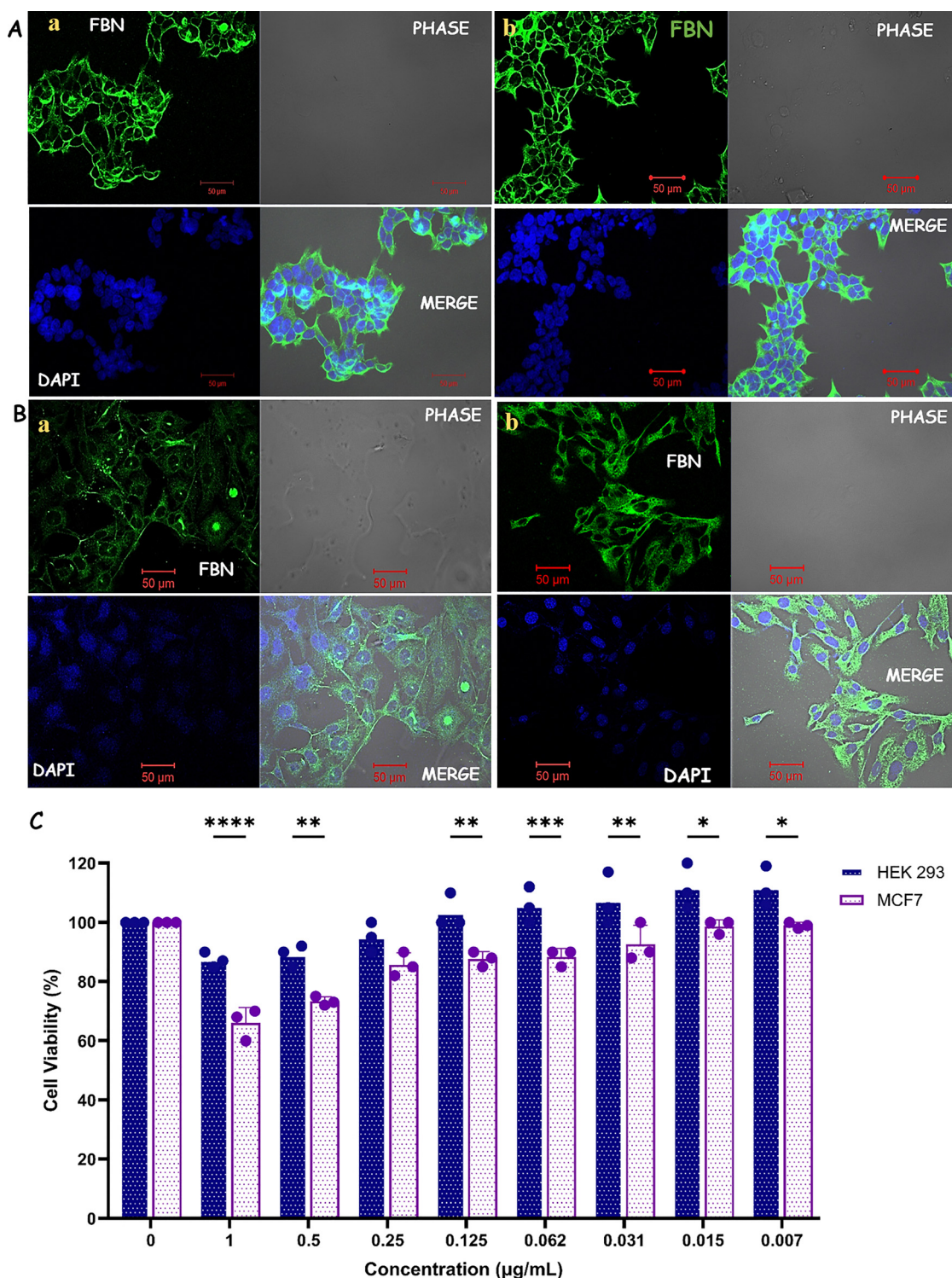
Fig. 6 Evaluation of Biocompatibility of poly-MAGC Hydrogel in HEK 293T and MCF-7 Cell Lines. (A) Representative fluorescence images depicting HEK 293T cells cultured for 24 hours: (a) control (without poly-MAGC hydrogel) and (b) treated with poly-MAGC hydrogel, stained with DAPI to evaluate nuclear and cellular morphology. (B) Representative fluorescence images illustrating MCF-7 cells cultured for 24 hours: (a) control and (b) treated with poly-MAGC hydrogel, stained with DAPI. (C) Dose-dependent assessment of cell viability in HEK 293T and MCF-7 cells following a 24-hour incubation with escalating concentrations of poly-MAGC hydrogel, as determined by the MTT assay. Cells were plated at a density of 2.5×10^4 cells per well in 96-well plates using RPMI medium. The results are expressed as mean $\pm$ SEM from three independent experiments.

The MTT assay, a standard method for evaluating cell metabolic activity, was employed to measure the cytotoxic effects of various hydrogel concentrations. The results of the MTT assay indicated that the hydrogel exhibited minimal toxicity across a broad range of concentrations. At a concentration of 250 μg mL^{-1}, the hydrogel demonstrated no adverse effects on cell viability in the HEK 293T and MCF-7 cell lines. Notably, even at a significantly higher concentration of 1 mg mL^{-1}, more than 80% of the cells remained viable, underscoring the material's low toxicity profile. This observation is particularly significant as materials with high cytocompatibility across a wide concentration range are crucial for applications where prolonged or high-dose exposure is required, such as in drug delivery systems or tissue engineering scaffolds. Interestingly, at a concentration of 250 μg mL^{-1}, the hydrogel material not only avoided cytotoxic effects but also promoted cell proliferation in all tested cell lines. As illustrated in Fig. 6, this enhancement in cell growth highlights the potential of the hydrogel as a supportive matrix for cellular activity, making it an excellent candidate for tissue engineering and wound healing applications.

Furthermore, the hydrogel demonstrated similar biocompatibility at 500 μg mL^{-1}, suggesting its suitability for applications requiring higher concentrations without compromising cell health. The findings underscore the hydrogel's high biocompatibility and its ability to maintain cell viability, even at elevated concentrations. This is a critical attribute for biomaterials intended for use in drug delivery, as materials must not only be effective in carrying and releasing therapeutic agents, but also be non-toxic to surrounding tissues.

Moreover, the observed promotion of cell proliferation further supports the potential of this hydrogel in regenerative medicine, where scaffolds must foster cellular growth and tissue formation.

Taken together, these results demonstrate that the poly-MAGC hydrogel possesses the desirable properties of low cytotoxicity and high biocompatibility, making it a promising candidate for a variety of biomedical applications. Future studies should explore the material's performance in *in vivo* models, as well as its ability to integrate with other functional biomolecules, to fully unlock its potential in drug delivery, tissue engineering, and wound healing.

Antibacterial activity

The antimicrobial efficacy of chemically synthesized poly-MAGC hydrogels against *E. coli* was evaluated using the drug diffusion method. The inhibition zones, indicative of bacterial growth suppression, were measured in millimetres (mm) and visually analyzed. Different concentrations of the hydrogel (2, 3, and 4 mg) were tested, as shown in the left panel of Fig. 7.

The results indicated that the hydrogel, in its current formulation, exhibited negligible antibacterial activity, as no significant inhibition zones were observed against Gram-positive and Gram-negative bacteria. This suggests that the poly-MAGC hydrogel lacks inherent bacteriostatic or bactericidal properties against *E. coli* and *E. faecalis*. To test the efficacy of drug absorption and slow-release properties of poly-MAGC, we first incubated 3, 6 and 9 mg of poly-MAGC hydrogels with 100 μg mL^{-1} of CB solution as per the methodology and placed them on Agar plates with *E. coli*, which is depicted in the right panel of Fig. 7. The corresponding inhibition zones were 21 mm, 26 mm, and 27 mm, demonstrating antibacterial efficacy. Pure CB was used as a positive control at concentrations of 20, 40, and 50 μg, as shown in the left panel of Fig. 7.
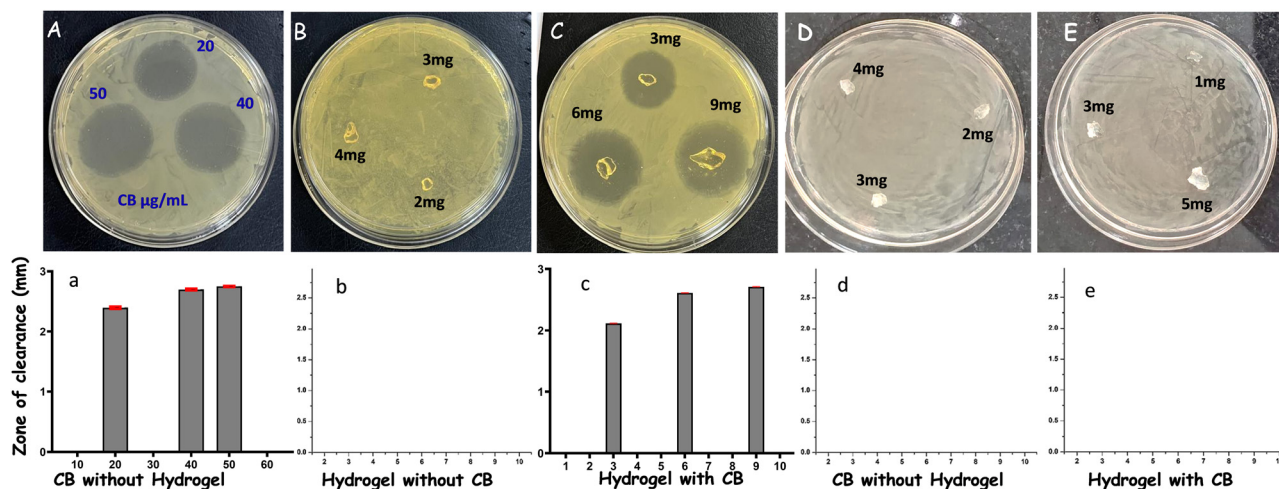

Fig. 7 Comparative antimicrobial activity of poly-MAGC hydrogels against *Escherichia coli* and *Enterococcus faecalis*. (A, a) Antibacterial activity of pure carbenicillin (CB) at concentrations of 20, 40, and 50 μg, showing a concentration-dependent increase in inhibition zones, with maximum activity at 50 μg. (B, b) poly-MAGC hydrogels without CB loading exhibited no significant inhibition zones, indicating negligible inherent antibacterial activity. (C, c) CB-loaded poly-MAGC hydrogels (3, 6, and 9 mg) displayed limited inhibition zones (2.1–2.7 mm), confirming partial antibacterial activity due to drug release from the hydrogel matrix. (D, d & E, e) poly-MAGC Hydrogels tested against *E. faecalis* showed no detectable inhibition zones, even with CB loading, suggesting that the hydrogel system is less effective against Gram-positive strains. Overall, results highlight that poly-MAGC hydrogels act primarily as passive carriers with low intrinsic antibacterial effects, while CB release governs antimicrobial performance.

The inhibition zones observed were 24 mm, 27 mm, and 27.5 mm, respectively, indicating a dose-dependent increase in antibacterial activity. A second set of CB concentrations (60, 80, and 100 μg) showed (Fig. S2) only a marginal increase in inhibition zones compared to 50 μg, suggesting that 50 μg represents an optimal concentration for effective bacterial killing. These findings highlight the strong antimicrobial activity of CB, even at moderate concentrations. The results indicated that 6 mg of hydrogel material was enough to show an optimal zone of inhibition. Although there was a slight increase in inhibition zones with higher hydrogel, the activity remained minimal. This result also indicates the drug release property of poly-MAGC, highlighting its potential use in wound therapy.

Overall, while CB demonstrated robust antibacterial properties, the poly-MAGC hydrogel in its current form was inadequate as a standalone antimicrobial agent. The drug-loaded hydrogel exhibited marginal activity, indicating potential as a drug delivery platform. Future studies should focus on enhancing the hydrogel's drug-loading capacity, optimizing release kinetics, and possibly modifying its chemical structure to improve interaction with bacterial membranes. Such efforts could pave the way for developing poly-MAGC hydrogels into effective antimicrobial delivery systems.

Experimental methods

Materials

Commercially available chemicals were used in this work are Methacrylic acid (MAA 99%), acryl amide (AAm) from was supplied from SRL. Gelatin from porcine skin (90–100 kDa), Chitosan low molecular weight ($\sim$150 kDa), potassium persulfate, carbenicillin, sodium hydroxide (NaOH 97.0%), sodium chloride (NaCl) and ethanol were obtained from Sigma Aldrich. All chemicals were used without further purification.

Synthesis of poly-MAGC

Poly-MAGC hydrogel was synthesized using a thermally induced free radical polymerization technique. Initially, 500 mg of MAA and 50 mg of AAm were dissolved in a solvent mixture comprising 0.2 mL ethanol, 0.5 mL distilled water, 8 mg NaOH, and 8 mg NaCl. This solution was sonicated for 5 minutes to ensure uniform dispersion of components. Subsequently, 1 mL of a 3% solution of gelatin and chitosan (prepared in equal proportions) was added to the sonicated mixture. The combined solution was subjected to vigorous stirring at 70 °C for 20 minutes to promote thorough interaction among the components. To initiate polymerization, 8 mg of potassium persulfate (KPS) was introduced, and the solution was stirred for an additional 3 minutes. The polymerization reaction was carried out by incubating the mixture in an oven set at 70 °C for 3 hours. Following this, the hydrogel was cooled on ice and stored at 4 °C for future applications. The hydrogel was dried using a freeze-drying technique to preserve its porous structure and ensure uniform drying. The synthesized hydrogel was characterized using Fourier-transform infrared (FTIR) spectroscopy to identify functional groups and verify chemical structures in the 4000–600 cm^{-1} range. To confirm the successful polymerization of monomers into the poly-MAGC hydrogel network, we performed ^{1}H NMR spectroscopy using methanol-d_4 as the solvent. The hydrogel morphology was evaluated using field emission scanning electron microscopy (FESEM), providing insights into its structural features.

Swelling nature and water retention

The swelling behaviour of poly-MAGC hydrogel was assessed by immersing 100 mg of dried hydrogel in buffer solutions of varying pH values (4.4, 5.4, 7.0, 7.4 (PBS), and 8.4) at a controlled temperature of 27 °C. The hydrogel samples were removed, carefully blotted to remove surface water, and weighed at pre-determined time intervals. The swelling ratio (SR), indicating the hydrogel's water absorption capacity, was calculated using the following formula:

$$\text{SR}\,(\%) = \left[\frac{W_s - W_d}{W_d}\right] \times 100 \qquad (1)$$

where W_s represents the weight of the swollen hydrogel, and W_d denotes the weight of the dried hydrogel. To evaluate the water retention capabilities of swollen hydrogels obtained from different pH levels (4.4, 5.4, 7.0, 7.4 (PBS), and 8.4) at 27 °C, the swollen hydrogels were exposed to ambient air conditions with approximately 40% relative humidity. The water retention ratio (WRR) was determined over time using the formula:

$$\text{WRR}\,(\%) = \left[\frac{W_s - W_d}{W_d \times \text{SR}}\right] \times 100 \qquad (2)$$

where W_s represents the weight of the swollen hydrogel, and W_d denotes the weight of the dried hydrogel.

Contact angle assessment

The wettability of the poly-MAGC hydrogel film was assessed through static water contact angle measurements. A $\sim$5 μL droplet of deionized water was placed on the hydrogel surface, and the spreading dynamics were recorded over time utilizing a goniometer fitted with a digital camera. Images were analyzed at various intervals: the pristine hydrogel surface without the droplet (A), a pure water droplet on an inert surface serving as a reference (B), the hydrogel surface immediately following droplet deposition ($\sim$6 s, C), and after 120 s (D). Contact angle values were calculated using drop shape analysis software, and the findings are compiled in Table S1 in SI. Each experiment was conducted in triplicate to ensure consistency.

BET experiment

The surface area and porosity of the freeze-dried hydrogel were assessed through Brunauer–Emmett–Teller (BET) nitrogen adsorption–desorption isotherm analysis. Before the measurements, the hydrogel was finely ground and subjected to vacuum degassing at 120 °C for 8 hours to remove any adsorbed moisture and volatile impurities. BET analyses were performed using a Quantachrome Autosorb iQ-XR surface area and pore

size analyzer (3 Stat., Viton; Serial No.: 1050041616) at a temperature of 77 K, with nitrogen serving as the adsorbate. Approximately 50 mg of the sample was analyzed for each run.

Carbenicillin loading and release

The encapsulation and controlled release of carbenicillin (CB) were studied to evaluate the hydrogel's drug delivery potential. For drug loading, 50 mg of hydrogel was incubated with 10 mL of a 0.0442 M CB solution for 16 hours at room temperature under dark conditions with continuous shaking. After incubation, the hydrogel was separated from the solution through filtration. The remaining unencapsulated CB in the solution was quantified using UV-vis spectroscopy. The encapsulation efficiency (EE) was calculated using the equation:

$$EE\,(\%) = \left[\frac{A - B}{A}\right] \times 100 \tag{3}$$

where A is the initial concentration of CB, and B is the concentration of unencapsulated CB in the supernatant. For drug release studies, the CB-loaded poly-MAGC was immersed in solutions of varying pH (4.4, 5.4, 7.0, 7.4 (PBS), and 8.4). The cumulative release of CB was monitored at specific intervals using UV-vis spectroscopy. The release profile was analysed to understand the hydrogel's drug delivery kinetics and pH responsiveness.

Enzymatic degradation

The enzymatic degradation of poly-MAGC hydrogel was evaluated by immersing samples (5, 10, 15 and 20 mg) in 10 mL PBS at 37 °C for 48 hours to achieve swelling equilibrium. Following this, collagenase was added to the solution, and the hydrogels were incubated for periods ranging from 2 hours to 14 days. At each time point, the hydrogels were removed, rinsed with PBS, lyophilized, and weighed. The degradation rate (DR) was calculated as follows:

$$DR\,(\%) = \left[\frac{W_0 - W_t}{W_0}\right] \times 100 \tag{4}$$

where W_0 is the initial weight of the hydrogel, and W_t is the weight of the hydrogel at time t.

Rheological characterization of poly-MAGC hydrogel

The viscoelastic and flow properties of the poly-MAGC hydrogel were characterized through amplitude sweeps, frequency sweeps, temperature ramps, time sweep and flow curves. For all rheological measurements, a cone-plate geometry of 25 mm with a gap size of 0.105 mm was used. This geometry was selected to ensure uniform shear distribution and minimize edge effects, which is particularly important for hydrogel characterization. The strain amplitude sweep, conducted with oscillatory strain ranging from 0.001% to 100% at 1 Hz, identified the linear viscoelastic (LVE) region where the storage modulus (G') and loss modulus (G'') remained constant, reflecting the hydrogel's structural stability. A frequency sweep within the LVE range ($\sim$0.2% strain) across angular frequencies from 0.01 to 400 rad s^{-1} revealed the elastic (G') and viscous (G'')

behaviour of the material over different timescales. To evaluate thermal effects, a temperature ramp from 27 °C to 60 °C at 5 °C min^{-1}, with a constant strain of 1% and fixed frequency, demonstrated the temperature-dependent viscoelastic properties. Time sweep (aging) rheology tests was conducted from 0 to 220 min at 27 °C to monitor how a material's viscoelastic properties evolve over time, offering valuable insights into its aging behaviour, structural stability, fatigue resistance, and potential degradation. Finally, viscosity measurements at 27 °C with shear rates from 0.001 to 100 rad s^{-1} confirmed the hydrogel's pseudoplastic (shear-thinning) behaviour, transitioning from Newtonian flow at low shear rates to non-Newtonian characteristics at higher rates. These results highlight the hydrogel's potential adaptability for applications requiring tailored viscoelastic and flow properties.

Cell culture studies

Human embryonic kidney (HEK 293T) and Michigan Cancer Foundation-7 (MCF-7) cell lines were cultured to assess the biocompatibility of the hydrogel. Cells were maintained in RPMI-1640 medium supplemented with 2 mM L-glutamine, 10% fetal calf serum (FCS), 100 IU mL^{-1} penicillin, and 100 μg mL^{-1} streptomycin. Cultures were incubated at 37 °C in a humidified atmosphere containing 5% CO_2.

Metabolic activity analysis

The hydrogel's impact on cellular metabolic activity was assessed using the MTT assay. Cells were seeded and allowed to adhere overnight. Hydrogel extracts were prepared at concentrations ranging from 1 mg mL^{-1} to 0.75 μg mL^{-1} in PBS. The cells were exposed to these extracts for 24 hours, after which MTT dye was added to the wells. Formazan crystals formed by metabolically active cells were dissolved in dimethyl sulfoxide (DMSO), and absorbance was measured at 570 nm (reference at 630 nm). Cell viability was calculated as a percentage of the control.

Antibacterial activity

The antibacterial activity of poly-MAGC hydrogel was assessed using the agar diffusion method. Drug-free hydrogels weighing 2, 3, and 4 mg were sterilized under UV light for 30 minutes. Another set of hydrogels, weighing 3, 6, and 9 mg, were also sterilized similarly and immersed in 100 μg mL^{-1} CB solution overnight at 4 °C, followed by three washes with PBS and subsequent UV sterilization. *Escherichia coli* DH5α and *E. faecalis* cultures with an optical density of 0.4–0.5 were uniformly spread on agar plates, after which the hydrogels were placed on the agar plates. The plates were incubated overnight at 37 °C, and zones of inhibition were measured. The actual inhibition zone was calculated by subtracting the hydrogel disc diameter from the total observed zone on the agar plate, in accordance with standard antimicrobial susceptibility testing guidelines (CLSI, 2020) to evaluate the antimicrobial activity of the hydrogels, comparing drug-free, CB-loaded, and CB-only treatments.

Conclusions

In conclusion, the poly-MAGC hydrogel created in this research demonstrates significant biocompatibility, mechanical robustness, and remarkable pH-responsive swelling, rendering it exceptionally appropriate for biomedical uses. The hydrogel exhibited a substantial drug loading capacity (0.0393 M, 89% efficiency) along with a controlled release profile under physiological conditions, which are vital for localized and sustained therapeutic delivery. Its ability to retain water guarantees extended hydration, which is crucial for applications in wound healing. Although the unmodified hydrogel displayed minimal antibacterial properties, the drug-loaded poly-MAGC successfully inhibited bacterial proliferation, thereby affirming its potential as a drug delivery system. In comparison to previously documented hydrogels, poly-MAGC presents the combined benefits of synthetic and natural polymers without the need for harmful chemical crosslinkers, underscoring its innovative nature. While the current study is confined to *in vitro* assessments, future investigations will aim to include *in vivo* testing in animal models. Overall, these results position poly-MAGC as a promising next-generation hydrogel for enhanced wound healing, drug delivery, and tissue engineering applications.

Author contributions

Ideation, experimental design, and experimental results analysis performed by A. K. and R. K. Antibacterial work helped by R. P. and S. V. edited final version by R. K. and P. K., S. V. R. K. K. helped in the chemical synthesis part. All authors have read and agreed to the published version of the manuscript.

Conflicts of interest

There are no conflicts to declare.

Data availability

The data supporting this article have been included as part of the supplementary information (SI). Supplementary information contains additional characterization data, including contact angle measurements, viscosity curves, and extended antibacterial assay results. See DOI: https://doi.org/10.1039/d5ma00564g.

Acknowledgements

References

1 M. Vigata, C. Meinert, D. W. Hutmacher and N. Bock, Hydrogels as Drug Delivery Systems: A Review of Current Characterization and Evaluation Techniques, *Pharmaceutics*, 2020, **12**, 1188.

2 D. B. Tripathy, Hydrogels: multifunctional biomaterials with versatile applications, *Polym.-Plast. Technol. Mater.*, 2023, **62**(18), 2403–2433, DOI: 10.1080/25740881.2023.2260885.

3 E. M. Ahmed, C. Meinert, D. W. Hutmacher and N. Bock, Hydrogel: Preparation, characterization, and applications: A review, *J. Adv. Res.*, 2015, **6**, 105–121, DOI: 10.1016/j.jare.2013.07.006.

4 C. M. Ninciuleanu, R. Ianchiş, E. Alexandrescu, C. I. Mihăescu, C. Scomoroşcenco, C. L. Nistor, S. Preda, C. Petcu and M. Teodorescu, The Effects of Monomer, Crosslinking Agent, and Filler Concentrations on the Viscoelastic and Swelling Properties of Poly(methacrylic acid) Hydrogels: A Comparison, *Materials*, 2021, **14**, 2305.

5 S. K. Swain and K. Prusty, Biomedical applications of acrylic-based nanohydrogels, *J. Mater. Sci.*, 2018, **53**(4), 2303–2325, DOI: 10.1007/s10853-017-1726-x.

6 E. J. Cozens, N. Roohpour and J. E. Gautrot, Comparative adhesion of chemically and physically crosslinked poly-(acrylic acid)-based hydrogels to soft tissues, *Eur. Polym. J.*, 2021, **146**, 110250.

7 V. Ugrinovic, V. Panic, P. Spasojevic, S. Seslija, B. Bozic, R. Petrovic, D. Janackovic and D. Veljovic, Strong and tough, pH sensible, interpenetrating network hydrogels based on gelatin and poly(methacrylic acid), *Polym. Eng. Sci.*, 2022, **62**(3), 622–636, DOI: 10.1002/pen.25870.

8 L. Hanyková, J. Šťastná and I. Krakovský, Responsive Acrylamide-Based Hydrogels: Advances in Interpenetrating Polymer Structures, *Gels*, 2024, **10**(2), 118.

9 M. Thippeswamy, M. Puttagiddappa, T. Demappa and N. Satyanarayan, Poly(acrylamide-*co*-acrylic acid) synthesized, moxifloxacin drug-loaded hydrogel: Characterization and evaluation studies, *J. Appl. Pharm. Sci.*, 2021, **11**(12), 023–033, DOI: 10.7324/JAPS.2021.1101205.

10 S. Heidari, F. Esmaeilzadeh, D. Mowla and S. Ghasemi, Synthesis of an efficient copolymer of acrylamide and acrylic acid and determination of its swelling behavior, *J. Pet. Explor. Prod. Technol.*, 2018, **8**(4), 1331–1340, DOI: 10.1007/s13202-017-0428-x.

11 T. Erceg, T. Dapčević-Hadnađev, M. Hadnađev and I. Ristić, Swelling kinetics and rheological behaviour of microwave synthesized poly(acrylamide-*co*-acrylic acid) hydrogels, *Colloid Polym. Sci.*, 2021, **299**(1), 11–23, DOI: 10.1007/s00396-020-04763-9.

12 D. Tripathy, Hydrogels: multifunctional biomaterials with versatile applications, *Polym.-Plast. Technol. Mater.*, 2023, **62**, 2403–2433, DOI: 10.1080/25740881.2023.2260885.

13 C. Gao, Z. Gao, Y. Wei, N. Luo, Y. Liu and P. Huo, Flexible Wood Enhanced Poly(acrylic acid-*co*-acrylamide)/Quaternized Gelatin Hydrogel Electrolytes for High-Energy-Density Supercapacitors,

ACS Appl. Mater. Interfaces, 2023, **15**(2), 2951–2960, DOI: **10.1021/acsami.2c18935**.

14 A. Jafari, S. Hassanajili, F. Ghaffari and N. Azarpira, Modulating the physico-mechanical properties of polyacrylamide/gelatin hydrogels for tissue engineering application, *Polym. Bull.*, 2022, **79**(3), 1821–1842, DOI: **10.1007/s00289-021-03592-2**.

15 N. Ma, X. Li, Z. Ding, J. Tao, G. Xu, Y. Wang, Y. Huang and J. Liu, A polyacrylic acid/polyacrylamide-based hydrogel electrolyte containing gelatin for efficient electrochromic device with outstanding cycling stability and flexible compatibility, *Eur. Polym. J.*, 2023, **190**, 112024, DOI: **10.1016/j.eurpolymj.2023.112024**.

16 D. Alemu, E. Getachew and A. K. Mondal, Study on the Physicochemical Properties of Chitosan and their Applications in the Biomedical Sector, *Int. J. Polym. Sci.*, 2023, **2023**(1), 5025341, DOI: **10.1155/2023/5025341**.

17 N. M. B. Ladeira, C. L. Donnici, J. P. de Mesquita and F. V. Pereira, Preparation and characterization of hydrogels obtained from chitosan and carboxymethyl chitosan, *J. Polym. Res.*, 2021, **28**(9), 335, DOI: **10.1007/s10965-021-02682-z**.

18 J. B. Safari, A. M. Bapolisi and R. W. M. Krause, Development of pH-Sensitive Chitosan-g-poly(acrylamide-*co*-acrylic acid) Hydrogel for Controlled Drug Delivery of Tenofovir Disoproxil Fumarate, *Polymers*, 2021, **13**(21), 3707.

19 S.-N. Li, B. Li, Z.-R. Yu, Y. Li, K.-Y. Guo, L.-X. Gong, Y. Feng, D. Jia, Y. Zhou and L.-C. Tang, Constructing dual ionically cross-linked poly(acrylamide-*co*-acrylic acid)/chitosan hydrogel materials embedded with chitosan decorated halloysite nanotubes for exceptional mechanical performance, *Composites, Part B*, 2020, **194**, 108046, DOI: **10.1016/j.compositesb.2020.108046**.

20 S. Aihua, X. Dai and Z. Jing, Tough and Self-Healing Chitosan/Poly(acrylamide-*co*-acrylic acid) Double Network Hydrogels, *Polym. Sci., Ser. A*, 2020, **62**(3), 228–239, DOI: **10.1134/S0965545X20030128**.

21 N. Falcone, T. Shao, N. M. O. Andoy, R. Rashid, R. M. A. Sullan, X. Sun and H.-B. Kraatz, Multi-component peptide hydrogels – a systematic study incorporating biomolecules for the exploration of diverse, tuneable biomaterials, *Biomater. Sci.*, 2020, **8**(20), 5601–5614, DOI: **10.1039/D0BM01104E**.

22 L. J. Marshall, S. Bianco, R. E. Ginesi, J. Doutch, E. R. Draper and D. J. Adams, Investigating multigelator systems across multiple length scales, *Soft Matter*, 2023, **19**(26), 4972–4981, DOI: **10.1039/D3SM00521F**.

23 E. Rosa, P. Pellegrino, M. Cascione, R. Rinaldi, E. Gianolio, C. Edwards-Gayle, I. W. Hamley, G. Morelli, A. Accardo and C. Diaferia, Cross-Link of Telechelic Diacrylate Polyethylene-Glycol in Peptide-Based Fmoc-FF Hydrogel Matrices, *ACS Appl. Polym. Mater.*, 2024, **6**(12), 7197–7208, DOI: **10.1021/acsapm.4c01059**.

24 E. J. Fischer, G. Storti and D. Cuccato, Aqueous Free-Radical Polymerization of Non-Ionized and Fully Ionized Methacrylic Acid, *Processes*, 2017, **5**(4), 83.

25 V. Ugrinovic, M. Milutinovic, B. Bozic, R. Petrovic, D. Janackovic, V. Panic and D. Veljovic, Poly(methacrylic acid)/gelatin interpenetrating network hydrogels reinforced by nano-structured hydroxyapatite particles—improved drug delivery systems, *Int. J. Polym. Mater. Polym. Biomater.*, 2024, **73**(6), 417–431, DOI: **10.1080/00914037.2022.2164281**.

26 V. Ugrinovic, M. Markovic, B. Bozic, V. Panic and D. Veljovic, Physically Crosslinked Poly(methacrylic acid)/Gelatin Hydrogels with Excellent Fatigue Resistance and Shape Memory Properties, *Gels*, 2024, **10**(7), 444, DOI: **10.3390/gels10070444**.

27 I. Z. Abidin, E. J. Murphy, G. W. Fehrenbach, N. Gately and I. Major, Chitosan-(poly)acrylic acid polyelectrolyte complexes: Enhanced mucoadhesion and sustained drug release in vaginal tablets, *Carbohydr. Polym. Technol. Appl.*, 2024, **7**, 100480, DOI: **10.1016/j.carpta.2024.100480**.

28 R. Parhi, Cross-Linked Hydrogel for Pharmaceutical Applications: A Review, *Adv. Pharm. Bull.*, 2017, **7**(4), 515–530, DOI: **10.15171/apb.2017.064**.

29 M. Rizwan, S. Rubina Gilani, A. Iqbal Durani and S. Naseem, Materials diversity of hydrogel: Synthesis, polymerization process and soil conditioning properties in agricultural field, *J. Adv. Res.*, 2021, **33**, 15–40, DOI: **10.1016/j.jare.2021.03.007**.

30 E. Siqueira, J. França, R. Souza, D. Leoterio, J. Cordeiro and D. Bogdan, Recent advances in the development of the physically crosslinked hydrogels and their biomedical applications, *Res. Soc. Dev.*, 2023, **12**, e18212843073, DOI: **10.33448/rsd-v12i8.43073**.

31 Y. Wang, J. Wang, Z. Yuan, H. Han, T. Li, L. Li and X. Guo, Chitosan cross-linked poly(acrylic acid) hydrogels: Drug release control and mechanism, *Colloids Surf., B*, 2017, **152**, 252–259, DOI: **10.1016/j.colsurfb.2017.01.008**.

32 L. Cui, Y. Yao and E. K. F. Yim, The effects of surface topography modification on hydrogel properties, *APL Bioeng.*, 2021, **5**(3), 031509, DOI: **10.1063/5.0046076**.

33 K. Odziomek, A. K. Drabczyk, P. Kościelniak, P. Konieczny, M. Barczewski and K. Bialik-Wąs, The Role of Freeze-Drying as a Multifunctional Process in Improving the Properties of Hydrogels for Medical Use, *Pharmaceuticals*, 2024, **17**(7), 949.

34 M. Thommes, K. Kaneko, A. V. Neimark, J. P. Olivier, F. Rodriguez-Reinoso, J. Rouquerol and K. S. W. Sing, Physisorption of gases, with special reference to the evaluation of surface area and pore size distribution (IUPAC Technical Report), 2015, **87**(9–10), 1051–1069, DOI: **10.1515/pac-2014-1117** (acccessed 2025-04-29).

35 J. Rouquerol; P. Llewellyn and F. Rouquerol, Is the bet equation applicable to microporous adsorbents? In *Studies in Surface Science and Catalysis*, ed P. L. Llewellyn, F. Rodriquez-Reinoso, J. Rouqerol, N. Seaton, Elsevier, 2007, vol. 160, pp. 49–56.

36 G. Crini and E. Lichtfouse, Advantages and disadvantages of techniques used for wastewater treatment, *Environ. Chem. Lett.*, 2019, **17**(1), 145–155, DOI: **10.1007/s10311-018-0785-9**.

37 B. S. Kaith, A. Singh, A. K. Sharma and D. Sud, Hydrogels: Synthesis, Classification, Properties and Potential

Applications—A Brief Review, *J. Polym. Environ.*, 2021, **29**(12), 3827–3841, DOI: **10.1007/s10924-021-02184-5**.

38 W. Feng and Z. Wang, Tailoring the Swelling-Shrinkable Behavior of Hydrogels for Biomedical Applications, *Adv. Sci.*, 2023, **10**(28), 2303326, DOI: **10.1002/advs.202303326**.

39 L. K. Tomar, C. Tyagi, Y. E. Choonara, P. Kumar and V. Pillay, Rheological and Swelling Behavior of pH Sensitive Hydrogel Particles, *APCBEE Proc.*, 2014, **9**, 192–196, DOI: **10.1016/j.apcbee.2014.01.034**.

40 M. Suhail, Y.-H. Hsieh, Y.-F. Shao, M. U. Minhas and P.-C. Wu, Formulation and In-Vitro Characterization of pH-Responsive Semi-Interpenetrating Polymer Network Hydrogels for Controlled Release of Ketorolac Tromethamine, *Gels*, 2021, **7**(4), 191.

41 Q. Lv, M. Wu and Y. Shen, Enhanced swelling ratio and water retention capacity for novel super-absorbent hydrogel, *Colloids Surf., A*, 2019, **583**, 123972, DOI: **10.1016/j.colsurfa.2019.123972**.

42 J. Wu, W. Xue, Z. Yun, Q. Liu and X. Sun, Biomedical applications of stimuli-responsive "smart" interpenetrating

polymer network hydrogels, *Mater. Today Bio*, 2024, **25**, 100998, DOI: **10.1016/j.mtbio.2024.100998**.

43 H. Li, J. Wang, Y. Luo, B. Bai and F. Cao, pH-Responsive Eco-Friendly Chitosan–Chlorella Hydrogel Beads for Water Retention and Controlled Release of Humic Acid, *Water*, 2022, **14**(23), 3913.

44 R. Andreazza, A. Morales, S. Pieniz and J. Labidi, Gelatin-Based Hydrogels: Potential Biomaterials for Remediation, *Polymers*, 2023, **15**(4), 1021.

45 B. Lawless, H. Sadeghi, D. Temple, H. Dhaliwal, D. Espino and D. Hukins, Viscoelasticity of articular cartilage: Analysing the effect of induced stress and the restraint of bone in a dynamic environment, *J. Mech. Behav. Biomed. Mater.*, 2017, **75**, DOI: **10.1016/j.jmbbm.2017.07.040**.

46 N. Ruß, *Rheology and thermodynamics of starch-based hydrogel-mixtures*. 2016.

47 M. V. Ghica, M. Hîrjău, D. Lupuleasa and C.-E. Dinu-Pîrvu, Flow and thixotropic parameters for rheological characterization of hydrogels, *Molecules*, 2016, **21**(6), 786.